ELSEVIER

Spectrochimica Acta Part A 53 (1997) 1285–1299

SPECTROCHIMICA ACTA
PART A

Limitations of ab initio molecular dynamics simulations of simple reactions: $F + H_2$ as a prototype

Antônio J.R. da Silva, Hsiu-Yao Cheng [1], Douglas A. Gibson, Kathy L. Sorge, Zhihua Liu [2], Emily A. Carter *

Department of Chemistry and Biochemistry, Box 951569, University of California, Los Angeles, CA 90095-1569, USA

Received 8 November 1996; accepted 22 November 1996

Abstract

We present the first use of ab initio molecular dynamics (AIMD) with correlated wavefunctions to study a gas phase reaction. Our benchmark system is the well-studied $F + H_2$ reaction. The neutral, unstable species FH_2 is created by removing an electron from an equilibrated anion $(FH_2)^-$, simulating the photoelectron spectroscopy experiments of Neumark and co-workers. These experiments attempt to probe the transition state (TS) region by creating a negative ion that may have a structure similar to the neutral reaction TS. We then follow the dynamics of the neutral system on its Born–Oppenheimer surface, both forward and backward in time, to see how close the anion equilibrium geometry truly is to the neutral TS for the $F + H_2 \rightarrow HF + H$ reaction. We then perform AIMD from the actual neutral TS for comparison. All electronic energy and gradient calculations are at the complete active space self-consistent field level. We find for this system that our level of approximation leads only to a qualitatively correct description. It allows us, however, to show that at finite temperature the anion geometry is markedly different from the neutral TS structure in that instantaneous electron detachment forms an FH_2 complex lying entirely in the reactants valley. We propose that analysis of the asymptotic fragments in the photodetachment experiment will almost invariably detect $F + H_2$ and very rarely $FH + H$, and we also discuss which conditions would lead to a different conclusion. © 1997 Elsevier Science B.V.

Keywords: Molecular dynamics; Prototype; Transition state

1. Introduction

The reaction $F + H_2 \rightarrow HF + H$ has been extensively studied in the past 25 years, both experimentally [1–11] and theoretically [10–20]. It is a prototypical gas phase exothermic exchange reaction ($\Delta H \simeq 1.4$ eV) [12] with a very small barrier [1–3] of ~ 40–90 meV. The simplicity of the reaction has allowed it to be studied in great

* Corresponding author. Tel./fax: +1 310 2064038; e-mail: eac@chem.ucla.edu

[1] Permanent address: Department of Chemistry, Tunghai University, Taichung, Taiwan 407, Taiwan, ROC.

[2] Present address: Molecular Simulation, 9685 Scranton Rd., San Diego, CA 92121, USA.

PII S0584-8539(96)01872-7

detail, being undoubtedly one of the best understood of all chemical reactions [12,18]. Most of the studies have focused on the calculation of the potential energy surface [12,13,18] (PES) as well as the analysis of the dynamics of the reaction [15–17,19] (i.e. the study of the system as it goes from the reactants valley to the products valley). Many theoretical analyses of beam scattering experiments have shown that it is very difficult to calculate an ab initio PES that gives good agreement with the experimental findings [12,18]. Moreover, to properly describe the barrier height and transition state (TS) region one has to use an ab initio method that includes the effects of electron correlation at a very high level [12,18], This of course implies that the method will be computationally very expensive. Recently [18] a PES has been calculated at ~ 700 points using the internally contracted multireference configuration interaction with Davidson correction (MRCI + Q) technique, and then it was fit to an analytic form. This PES was then used to perform quasi-classical [15] and quantum dynamical [17,19] simulations of the $F + H_2 \rightarrow HF + H$ reaction and of the photoemission TS spectroscopy experiments of Neumark and collaborators [10,11,20].

In these photoemission experiments [9–11] the $(FH_2)^-$ is initially prepared rotationally cold ($T_{rot} \leq 50$ K), in its electronic ground state, and at a vibrational temperature of less than 150 K (D.W. Arnold, private communication). The electron is then photodetached and its kinetic energy is analysed (photoelectron spectroscopy). The idea is that if the anion has an equilibrium geometry similar to the TS for the neutral molecule, the photoelectron spectrum will give information about the TS [21,22]. In other words, the anion would allow the system to be effectively 'trapped' in the TS so one could perform TS spectroscopy.

All the theoretical analyses of these photodetachment experiments for the FH_2 system so far have been quantum dynamical simulations [10,11,20] where an initial wavepacket is propagated on the neutral PES. The advantage of these methods is that they include quantum mechanical effects like tunneling, which might be important in the $F + H_2 \rightarrow HF + H$ reaction because of the light H atoms. However, these methods have the disadvantage that they require the knowledge of the global PES and that they can deal only with a small number of degrees of freedom. For the present case these requirements are not a problem because of the simplicity of the system. However, for a more complex system, it may be prohibitively costly to perform such calculation.

A possible alternative to study the dynamics of atomic motion is to use classical molecular dynamics (MD) [23]. In these simulations the nuclei are considered to be classical particles with trajectories calculated through the solution of Newton's equations. Most often the forces on the nuclei are calculated using an analytic fit to the PES around well defined (usually equilibrium) geometries. However, in situations where bonds are broken and electronic configurations vary during the simulation these analytic potentials are typically not accurate enough even for a qualitative description. One option is to use ab initio methods to calculate the forces. This method is known as ab initio molecular dynamics (AIMD) and it is precisely the method that we are going to employ in the present work. Some of its advantages are: (i) it requires only a local knowledge of the PES; (ii) is flexible enough to deal with bond breaking and making; (iii) in principle, has no limits in the number of degrees of freedom that can be treated; and (iv) gives a very clear picture of the dynamics. The main disadvantages are that: (i) it does not include quantum mechanical effects in the motion of the nuclei, and cannot, for example, describe tunneling; (ii) it is purely adiabatic as formulated here (i.e. it does not allow the simultaneous description of multiple electronic states in the dynamics) [24]; and (iii) it is expensive, which limits gathering of decent statistics.

We have developed in our group both Car-Parrinello [25] and Born-Oppenheimer AIMD methods, and applied both methods to the study of small clusters at different levels of approximation for the electronic wavefunction [26]. In this work we are going to use the Born-Oppenheimer AIMD method. This means that at every time step the electronic wavefunction is fully optimized, which keeps the system always on the Born–Oppenheimer surface. Because we are performing an ab initio electronic structure calcula-

tion at every time step, both for the energy and for the gradients, the method can become computationally very expensive. Therefore, the approximation used to calculate the electronic wavefunction of the system will necessarily depend on the size of the system under study.

One could argue that because there exists already a PES for the FH_2 system calculated at a very high level of ab initio theory, which allowed detailed quantum dynamical calculations to be done, there is no point in performing a classical AIMD simulation. However, exactly because these previous calculations exist, the $F + H_2 \rightarrow HF + H$ reaction is a perfect benchmark system to assess the AIMD method. Also, because it is very difficult to accurately calculate the PES for the FH_2 system at the ab initio level, this is a very stringent test for the performance of the AIMD method. As we will show, the results obtained from our AIMD simulation give a qualitatively correct description at best. We are limited by the accuracy of available forces; one cannot calculate explicit analytic forces at the level of theory to which the very accurate PES was calculated (MRCI + Q). This does not mean that AIMD simulations will always only provide a qualitative understanding, but quantitative aspects will be highly dependent on the system and the extent to which dynamic correlations are important. In the next section, we discuss the way we are going to calculate the wavefunction and forces, i.e. our ab initio level. In section 3 we describe the way we are going to use the AIMD method to study electron photodetachment and present the results of the simulation. A discussion of the results is given in Section 4, followed by the conclusions.

2. Static properties

The method we have chosen to calculate the electronic energy and gradient for our AIMD simulations is the complete active space self-consistent field (CASSCF) level. Even though it is known that a MRCI + Q calculation really has to be performed on top of the CASSCF calculation to obtain an accurate PES, this will not be done here because of the reasons discussed in the last paragraph.

The Gaussian basis set for the H atoms uses the s functions from the Dunning augmented correlation consistent (cc) polarized valence triple-ξ (cc-pVTZ) [6s|4s] basis [27] and one polarization function ($\zeta_p = 0.739$). The basis set for the F atom consists of the s and p functions from the Dunning's augmented cc-pVTZ [11s6p|5s4p] basis [27] with one added polarization function ($\zeta_d = 1.63$). The resulting basis has a total of 36 (the s combination of the d functions on the F atom is deleted from the calculation) contracted basis functions. Our active space contains a total of seven orbitals, five of symmetry a′ and two of a″ symmetry (a′ and a″ label the irreducible representations of the point group C_s). The fluorine 1s and 2s orbitals (symmetry a′ in C_s) were kept doubly occupied in all configurations, although their SCF coefficients were fully optimized in the CASSCF wavefunction optimization (inactive space). In the active space of the reference configuration, there are three occupied a′ orbitals and one occupied a″ orbital. In the reactants channel, the a′ orbitals correspond to the H_2 bonding and F p_z and p_y orbitals. The a″ correspond to the F p_x. The active virtual a″ orbital is a F p'_x, and the two a′ virtuals are combinations of the H_2 anti-bonding and F p_z and p'_y orbitals. This choice of active space is similar to Bauschlicher et al.'s (322) choice [13], which they use as a starting point for a MRCI calculation. As discussed by Bauschlicher et al. [13], the third virtual a′ coming from the above orbitals is only weakly occupied and of the same importance as the $2\sigma_g$ orbital in H_2. Therefore, the virtual space should include either three or five virtual a′ orbitals (which would be the (522) active space of Bauschlicher et al. [13]). For the $(FH_2)^-$ calculations, there are eight valence electrons correlated in these seven active orbitals, with a total of 260 configurations state functions (CSFs). For FH_2 there are seven electrons correlated in the seven active orbitals, which gives 404 CSFs.

With the above approximations, we used HONDO [28] to optimize the $(FH_2)^-$ geometry. The results are shown in Table 1. Comparison with the results of Nichols et al. [29] show that we are in very good agreement with their CASSCF calculation for ten correlated electrons in nine

orbitals (instead of our eight electrons in seven orbitals). However, when we compare with their CCSD(T) result we see that the CASSCF F–H bond length is much larger (by ~ 0.31 Å).

For the neutral molecule, we used the Ridge Method [30] (using HONDO [28] to calculate energies and gradients) to locate the saddle point for the $F + H_2 \rightarrow FH + H$ reaction, and its geometry is also reported in Table 1. If we compare our results with the recent MRCI + Q calculation by Stark and Werner [18] (and previous results by other groups reported in their Table 7), we see that our F–H bond distance is a bit too short (by ~ 0.1 Å) and our H–H bond distance is slightly long (by ~ 0.03 Å). Our TS geometry is slightly bent, in agreement with what is believed to be the real situation for this reaction [18], but our F–H–H angle is too large. We obtain an F–H–H angle of 173.6° whereas the values reported in Table 7 of Stark and Werner's paper [18] are $\sim 120°$. For the classical barrier height, we obtain a value of 325 meV, which is much larger than the values (~ 40–90 meV) obtained at higher levels of calculation (see Table 7 of Stark and Werner [18] for a compilation of calculated values for the energy barrier).

In summary, at our level of approximation, the anion is better represented as a $[(F^-)H_2]$ complex rather than $(FH_2)^-$, which results in a very large F–H bond distance (we obtain a F–H bond distance of 1.997 Å whereas Nichols et al. [29] obtain 1.690 Å) and a H–H bond distance a little shorter (ours is 0.759 Å whereas Nichols et al. [29] is 0.770 Å) and very close to our H_2 equilibrium geometry (H–H bond distance of 0.760 Å). When we compare our calculated F–H bond distance in the anion with the F–H bond distance for the neutral TS (the F–H bond length is larger in the anion by ~ 0.56 Å), we see that our anion equilibrium geometry is not similar to the TS geometry and is much closer to the entrance channel of the $F + H_2 \rightarrow HF + H$ reaction. On the other hand, as will be discussed in more detail later (see Section 4), the MRCI + Q structure of Stark and Werner [18] for the FH_2 TS also shows very different geometrical parameters than for $(FH_2)^-$ (namely $(FH_2)^-$ is linear and the FH_2 TS is very bent), again leading to the conclusion that $(FH_2)^-$ is not near the FH_2 TS, but for different reasons.

Table 1
Geometries for the $(FH_2)^-$ anion and the FH_2 saddle point($[FH_2]‡$)

System	R_e(F–H)	R_e(H–H)	θ_e(F–H–H)
$(FH_2)^-$	1.997	0.759	180
$(FH_2)^-$ [a]	1.999 (1.690)	0.758 (0.770)	180 (180)
$[FH_2]‡$	1.438	0.792	173.6
$[FH_2]‡$ [b]	1.546	0.771	119

All bond distances are in Å and bond angles in degrees.
[a] CASSCF results from Ref. [29]; CCSD(T) results from Ref. [29] shown in parentheses.
[b] MRCI + Q data from Ref. [18].

3. Dynamic simulations

All the simulations are done using the method of Born–Oppenheimer AIMD. By that we mean that the nuclei are treated as classical particles and are propagated according to Newton's equations of motion:

$$M_I \ddot{R} = -\frac{\partial E}{\partial R_I} \tag{1}$$

where M_I are the atomic masses, R_I are the nuclear coordinates, and E is the total potential energy. All the forces are calculated as the negative of the gradient of the Born–Oppenheimer PES for the ground state of the system as a function of the nuclear displacements. All the gradients and the PES calculations are performed at the CASSCF level using HONDO [28], as discussed in the previous section, which is interfaced to our molecular dynamics code. The method is named Born–Oppenheimer AIMD, as opposed to Car–Parrinello AIMD, because at each time step the wavefunction is fully converged, which keeps the system always on the Born–Oppenheimer surface. For all the trajectories reported here the equations of motion are integrated using the velocity-Verlet [31] algorithm with a time step of 0.24 fs (10 a.u.).

Our approach to studying the electron photodetachment experiments is the following: (1) first the

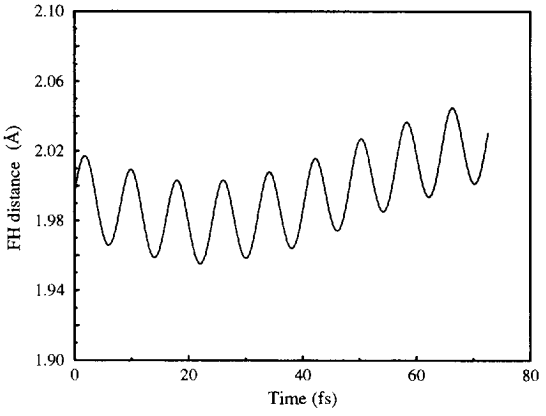

Fig. 1. F–H bond length (Å) for the anion trajectory Run_1^{an} as a function of time.

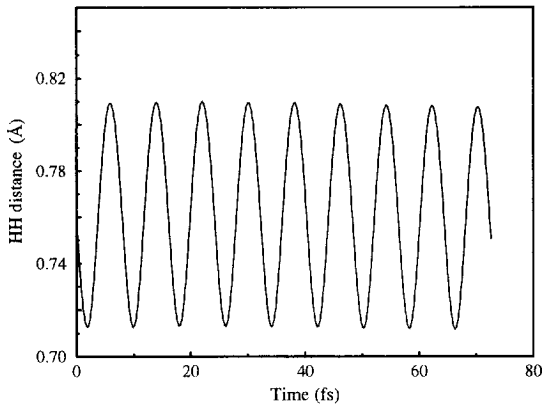

Fig. 2. H–H bond length (Å) for the anion trajectory Run_1^{an} as a function of time.

anion is propagated around its equilibrium geometry for a given amount of time (~ 80 fs); (2) at time intervals of ~ 12 fs along the anion trajectories, an electron is removed from the system; (3) the atomic coordinates and velocities at these times are used as initial conditions to propagate the molecule on the neutral Born–Oppenheimer surface. This procedure has the effect of mimicking the photodetachment experiment, assumed as a sudden vertical transition from the anion PES onto the neutral PES; (4) the trajectories are propagated both forward and backward in time starting from the initial conditions described in (3). This is done in order to see how close to the TS geometry the anion was before the electron was photodetached; and (5) the asymptotic fragments are analysed and their translational, rotational and vibrational energies calculated.

The initial geometry for the anion is its equilibrium geometry, and the initial velocities for each atom are randomly chosen from a Boltzmann distribution at 100 K, which is similar to the temperature used in the experiments (D.W. Arnold, private communication). The velocities are readjusted to set the total linear and angular momentum of the system to zero, and are then rescaled to give an initial temperature 100 K. Two anion trajectories were used in the present work, and they will be referred as Run_1^{an} and Run_2^{an} from now on. Figs. 1 and 2 present the F–H and H–H bond lengths, respectively, for Run_1^{an} as a function of time, whereas Figs. 3 and 4 present the same data for Run_2^{an}. When we compare Run_1^{an} and Run_2^{an}, we see that in Run_1^{an} the H–H bond is more excited than in Run_2^{an}, whereas the F–H bond is more excited in Run_2^{an} than in Run_1^{an}. This is a consequence of the random choice of initial velocities, and as will be shown later, it has an important effect in the distribution of energy among the asymptotic fragments that result from the electron photodetachment.

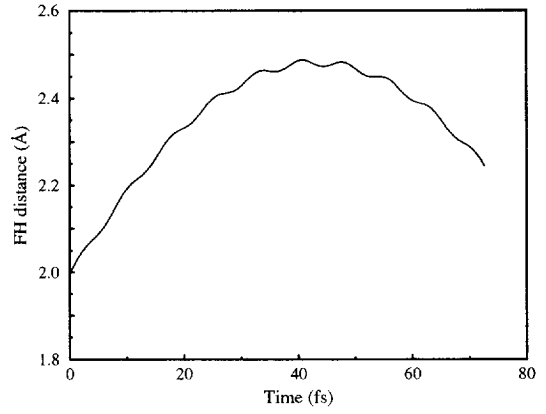

Fig. 3. F–H bond length (Å) for the anion trajectory Run_2^{an} as a function of time.

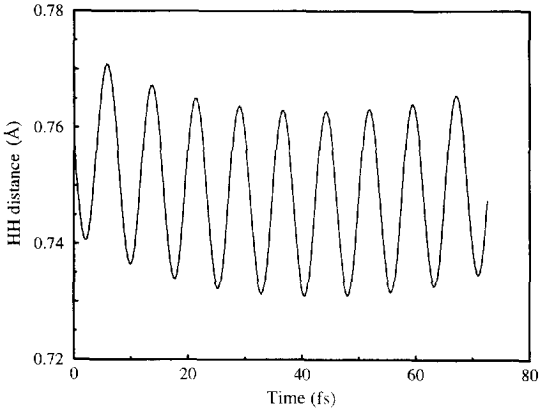

Fig. 4. H–H bond length (Å) for the anion trajectory Run_2^{an} as a function of time.

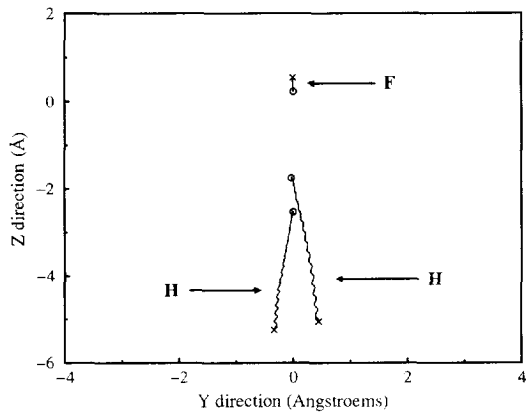

Fig. 5. Trajectory number 3 from Table 3 of the F and H atoms on the neutral PES after electron removal from an equilibrated $(FH_2)^-$ has occurred. The final fragments are $F + H_2$. Circles indicate $t = 0$ positions, crosses indicate final positions.

3.1. FH_2 trajectories from $(FH_2)^-$

Ten trajectories were calculated according to the above procedure. Six trajectories were selected from Run_1^{an} and four from Run_2^{an}. Each one was propagated ~ 120 fs in each direction, which was enough time for the fragments of the reaction to be well separated. The asymptotic fragments obtained for all ten trajectories are reported in Table 2, where we see that at all points in time the system is in the reactants valley, $F + H_2$. To analyze these trajectories, we note that the atomic motion happens all in a plane, which we have chosen to be the (yz) plane. The anion is initially aligned along the z axis, and because the initial angular and linear momentum are set to zero the atoms can only vibrate or bend around their equilibrium positions. A typical forward propagation is shown in Fig. 5. Each curve in this figure represents the trajectory performed by one of the atoms in the (yz) plane as the FH_2 complex dissociates. As can be seen, the final fragments for this particular case are an F atom and an H_2 molecule. As mentioned before, the FH_2 starts the trajectory on the neutral PES in an almost linear configuration, as indication by the circles in Fig. 5. As time proceeds the F atom and the H_2 molecule break apart. The vibrational motion of the H_2 molecule is reflected in the wavy pattern of the H atoms trajectories. The H_2 molecule also acquires rotational motion, which is clearly seen in Fig. 5 by the fact that at the end of the simulation, marked by the crosses in Fig. 5, the H_2 molecule is almost perpendicular to its original orientation, i.e. it lies almost entirely along the y direction.

Table 2
Asymptotic fragments obtained for the forward and backward propagation in the neutral PES after electron removal from $(FH_2)^-$

Run	Forward	Backward
$T = 100$ K		
1–10	$F+H_2$	$F+H_2$
$T = 1600$ K		
1	$HF+H$	$HF+H$
2	$F+H_2$	$F+H_2$
$T = 2000$ K		
1	$F+H_2$	$HF+H$
2	$F+H_2$	$F+H_2$
3	$HF+H$	$F+H_2$
4	$HF+H$	$HF+H$

The H_2 center-of-mass (COM) acceleration components along the y and z directions, for the trajectory shown in Fig. 5, are shown in Fig. 6. As can be noted, there is a large impulsive force along the z direction corresponding to the F–H bond breaking. After 40 fs the H_2 molecule is completely detached and moves freely. The y

component of the H_2 COM acceleration shown in Fig. 6 is much smaller than the z component, which implies that the H_2 COM final kinetic energy is going to be much larger than the final H_2 rotational energy.

These results are typical of all trajectories studied, and the calculated asymptotic energies for each trajectory are reported in Table 3. The first six rows for the 100 K data in Table 3 are for neutral complexes created from the anion along Run_1^{an}, and the last four rows for the 100 K data are for neutral complexes created from the anion along Run_2^{an}. The first thing to note is that the fragments from Run_1^{an} have a larger final H_2 COM kinetic energy and a much larger H_2 vibrational energy when compared with the fragments from Run_2^{an}. This can be easily understood from Figs. 1–4. In Run_1^{an} the F–H bond is less stretched than in Run_2^{an}. This makes the repulsive force larger when originating from Run_1^{an}. As a consequence the F atom and H_2 molecule will have more kinetic energy when originating from Run_1^{an}. On the other hand the H–H bond is more excited in Run_1^{an} than in Run_2^{an}. This will result in H_2 molecules with higher vibrational energy when originating from Run_1^{an}, as is observed. This shows that the anion trajectory has a large influence in the outcome of the reaction in the neutral PES, and a quantitative analysis requires averaging over many anion trajectories, which at this point is prohibitive. As our study is meant to be mostly illustrative, we use only these two anion trajectories. Note also in Table 3 that the H_2 COM kinetic energy is always larger than the F atom kinetic energy by a factor of ~ 9.5. This results because we have chosen the initial total linear momentum to be zero. As the system is isolated, the total linear momentum will be zero at all times, and therefore the H_2 COM linear momentum is always equal and opposite to the F atom linear momentum. The consequence is that $KE_{COM} = (M_F/M_{H_2})KE_F$, where KE_{COM} is the kinetic energy of the H_2 COM, KE_F is the F atom kinetic energy, M_{H_2} is the mass of the H_2 COM, and M_F is the mass of the F atom. This results in $KE_{COM} = 9.5KE_F$, in agreement with the data from Table 3.

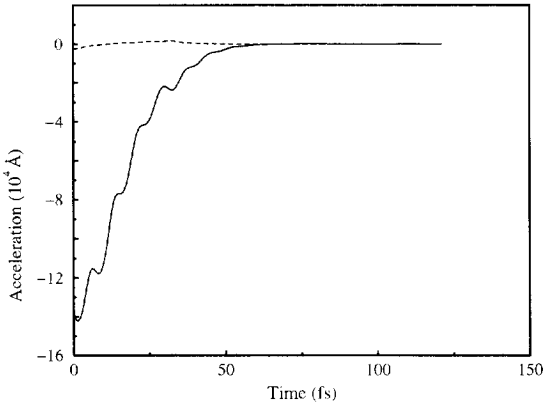

Fig. 6. The y (dashed line) and z (solid line) components of the H_2 center-of-mass acceleration as a function of time for the trajectory of Fig. 5.

Let us now consider how the energy partitioning given in Table 3 compares with a thermal Boltzmann distribution. The total thermal-energy content of the anion molecule is $3\ k_BT$, where k_B is the Boltzmann constant. This is so because we imposed zero total linear and angular momentum. This energy is divided between the three normal modes of vibration of the anion, which consist basically of a (F^-)–H_2 stretching, a H_2 stretching, and a F–H–H bending motion, with k_BT per mode. This gives ~ 8.6 meV per mode, or a total of ~ 25.9 meV of thermal energy. When the electron is photodetached and the molecule is brought to the neutral PES, we find that for the Run_1^{an} it lands at positions that are ~ 80–110 meV higher in energy than the bottom of the reactants valley (minimum energy for the $F + H_2$ system), whereas for Run_2^{an} it lands at positions that are ~ 20–40 meV higher (it is closer to the bottom of the valley because of the larger FH bond). These numbers should be compared with our CASSCF barrier for the reaction, which is ~ 325 meV. As we can see, the molecule excited to the neutral PES from the anion is much closer to the bottom of the reactants valley than the TS. From these numbers, we conclude that the total energy that the neutral molecule has before breaking apart is ~ 106–136 meV for trajectories originating from Run_1^{an}, and ~ 46–66 meV for trajectories originating from Run_2^{an}. This is in good agreement with the data from Table 3 for the trajectories originated from the anion Run_1^{an},

Table 3
Asymptotic energies (meV) for the fragments reported in Table 2

Run	Forward				Backward			
	KE_{atom}	KE_{COM}	E_{vib}	E_{rot}	KE_{atom}	KE_{COM}	E_{vib}	E_{rot}
$T = 100$ K								
1	8.5	81.1	38.2	0.3	8.3	78.8	43.6	4.1
2	7.5	71.6	36.5	14.0	8.4	80.1	34.9	4.7
3	8.5	80.4	40.8	2.3	7.4	70.4	43.4	13.4
4	7.6	72.4	35.8	6.5	8.1	77.2	32.0	0.5
5	7.0	66.1	41.3	11.0	6.8	64.6	41.3	12.7
6	7.4	70.2	36.3	2.1	7.2	68.0	36.4	4.5
7	2.0	18.6	1.2	0.02	2.0	18.6	1.2	0.5
8	1.6	15.6	10.1	4.4	1.9	17.7	10.0	0.9
9	2.8	26.2	2.5	5.4	3.1	29.7	2.5	0.3
10	5.8	55.0	5.2	2.5	7.1	67.3	5.0	0.3
Average	5.9	55.7	24.8	4.9	6.0	57.2	25.0	4.2
σ[a]	2.6	24.4	16.6	4.3	2.5	23.8	17.1	4.8
$T = 1600$ K								
1	108.8	5.4	2639.5	16.1	95.2	4.6	2340.2	19.3
2	16.0	151.5	435.4	73.5	16.5	156.3	435.4	70.8
$T = 2000$ K								
1	45.7	434.6	108.8	1.0	653.1	32.7	1387.8	127.9
2	6.7	63.4	870.8	62.6	9.3	87.9	870.8	29.2
3	89.8	4.6	2040.9	2.3	12.2	114.3	29.9	9.8
4	517.0	25.6	979.6	680.3	544.2	26.9	1333.4	326.5

KE_{atom} is the final kinetic energy for the atomic fragment, KE_{COM} is the final kinetic energy of the center-of-mass of the molecular fragment, E_{vib} its final vibrational energy and E_{rot} its final rotational energy.
[a] σ, standard deviation.

but not so good for the trajectories originated from the anion Run_2^{an}. For Run_2^{an} the thermal average is probably smaller than 3 k_BT. This shows again that it is important to do a large sampling of the initial states to wash out the effects of the fluctuations and to obtain quantitative results. On the other hand, it is likely that the experiments with which these simulations would be compared are not truly at equilibrium, and hence thermal averages may not be observed anyway.

The H–H bond length has a negligible change when going from the anion equilibrium geometry to the H–H equilibrium bond length (a change of ~ 0.001 Å), and therefore we would expect the final average vibrational energy of the H_2 molecule should be only k_BT, i.e. the same amount as in the H–H stretching mode in the anion. From Table 3 we see that the average H_2 vibrational energy that we obtain is much higher than k_BT (~ 25 meV instead of ~ 9 meV). However, the standard deviation is very large. In fact, if we average separately the first six trajectories (that originate from Run_1^{an}) we obtain for the H_2 vibrational energy the value of ~ 38 meV, whereas if we average the last four trajectories (that originate from Run_2^{an}), we obtain ~ 5 meV for the H_2 vibrational energy. As one can see one value is much higher than k_BT whereas the other is smaller. Therefore our sampling is still not good enough, and probably if we sampled more anion trajectories, the average H_2 vibrational energy would come closer to k_BT. The F–H–H anion bending motion will give rise to the rotational motion of the H_2 molecule. In analysing our trajectories, we observed that the angular momen-

tum associated with the rotational motion of the H_2 molecule is basically cancelled by the angular momentum associated with the H_2 COM motion (remember that the total angular momentum is zero). This means that the contribution of the F atom to the total angular momentum is negligible. The k_BT thermal energy associated with the F–H–H bending mode will be roughly equally divided between the rotation and translation of the H_2 molecule. This would give $0.5\ k_BT \simeq 4.3$ meV for $T = 100$ K, as thermal energy for the H_2 rotational motion. Comparison with the average H_2 rotational energy from Table 3 shows that the rotational energy is probably purely thermal, i.e. at our level of approximation, the rotational degree of freedom for the H_2 molecule does not seem to be coupled to the reaction coordinate. One would expect this because the neutral PES is relatively flat and the anion is far from the slightly bent TS region.

The k_BT thermal energy associated with the (F^-)–H_2 stretching will be divided among the F atom translational motion and the H_2 COM motion. With the requirement that $KE_{COM} = 9.5KE_F$, and the $0.5\ k_BT$ from the F–H–H bending motion that went into the H_2 COM translation, we obtain that $KE_{COM} = 1.36\ k_BT \sim 11.7$ meV and $KE_F = 0.14\ k_BT \sim 1.2$ meV. From Table 3 we see that both the F atom kinetic energy and the H_2 COM kinetic energy are significantly larger than these thermal values. This implies that these are the coordinates most strongly coupled to the reaction coordinate. This is expected because the anion lands on the neutral PES is regions that are very close to the bottom of the $F + H_2$ valley, i.e. the H–H bond distance is basically at its equilibrium value, and the potential is very flat with respect to the F–H–H bending angle. Therefore, the F atom and the H_2 COM are the only coordinates to which energy is transferred as the FH_2 rolls down the PES towards the bottom of the reactants valley (i.e. as it breaks apart into $F + H_2$).

A few trajectories were also calculated for the anion initially at 1600 and 2000 K. The objective was to allow the anion (specially the anion F–H bond) to probe the neutral TS region, and to allow the system the possibility of 'climbing' the reaction barrier. The results are also reported in Tables 2 and 3. We see from Table 2 that at 1600 K, distortion in the anion can result in formation of $HF + H$ or $F + H_2$, but that neither can be classified as reactive trajectories, since in neither trajectory was one molecule converted to the other (i.e. the atoms were always either in the products' or reactants' valley). By increasing the temperature to 2000 K, we see that true reactive trajectories can now occur, indicating that true classical barrier crossing could occur on the CASSCF PES at 2000 K.

3.2. FH_2 trajectories from the saddle point

We now want to compare the neutral system trajectories that started from the anion geometry after electron detachment with trajectories that started from the true transition state geometry. To do so we have performed also ten simulations that were propagated both forward and backward in time using the FH_2 TS geometry as their initial set of atomic coordinates. The initial velocities were the same initial velocities used in the simulations discussed above (the anion velocities directly before the electron detachment), adjusted in such a way that the total linear and angular momentum were zero. Fig. 7 shows a typical trajectory. In this particular case, the final fragments are an HF molecule and an H atom. The motion again

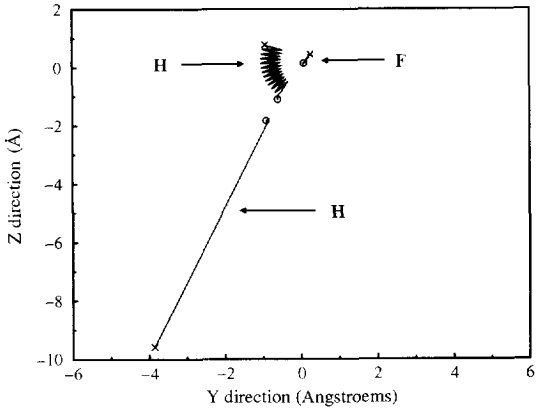

Fig. 7. Trajectory number 6 from Table 5 of the F and H atoms on the neutral PES starting from the neutral saddle point and where the final state is HF + H. Symbol conventions are as in Fig. 5.

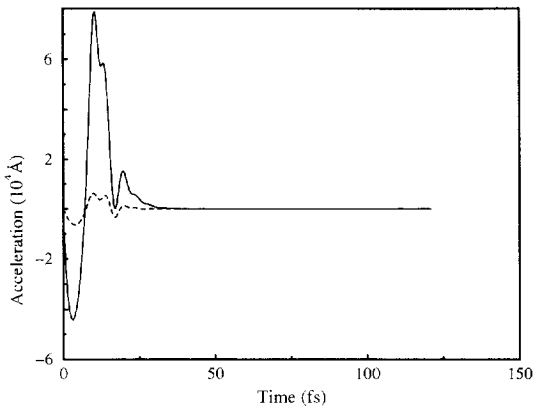

Fig. 8. The perpendicular (dashed line) and parallel (solid line) to the initial geometry (the neutral TS geometry) components of the HF center-of-mass acceleration as a function of time for the trajectory of Fig. 7. See text for detailed definition of perpendicular and parallel directions.

happens in the (yz) plane, but the FH_2 TS is not initially positioned along the z direction, as shown by the circles in Fig. 7. The vibrational motion of the HF molecule is characterized by the zig-zag motion of the H atom, and its rotational motion can be noted by the fact that the final geometry (indicated by the crosses) for the HF molecule is almost perpendicular to its initial geometry. The HF COM acceleration along the directions parallel and perpendicular to the FH_2 initial geometry for this trajectory are shown in Fig. 8. Because the initial geometry, i.e. the neutral TS, is not linear, we cannot clearly define perpendicular and parallel directions. By parallel we mean the direction defined by the initial vector pointing from the F atom to the H atom that is going to detach, and by perpendicular we mean perpendicular to this direction in the (yz) plane. When compared to Fig. 6, we see that the y-component is not as small, probably because of the bent structure of the saddle point. Moreover, it takes less time for the H–H bond to break ($\sim$ 30 fs) than the H–F bond, as expected from the exothermicity of this reaction.

All the trajectories starting from the neutral TS can be analysed in the same way as before, and the results are presented in the Tables 4 and 5. The first thing to note is that *all* the trajectories that start from the TS are *reactive* trajectories (meaning they start on one side of the barrier at early times and end up on the other side at late times), as they should be since there is no intrinsic mechanism that would drive recrossing of the barrier. This is in stark contrast to the trajectories from the simulated photodetachment where *none* were reactive at 100 K.

Let us first compare the results from Table 5 for the $F + H_2$ outcome of the reaction with the results from Table 3. We first not that the F and H_2 COM kinetic energies are much larger for the trajectories starting from the true neutral TS. This is expected because, as discussed before, these are the coordinates most strongly coupled to the reaction coordinate, and the main effect of starting from the true TS is that the FH_2 will roll down from the top of the barrier as it breaks apart. Therefore more energy will be transferred to these coordinates. We actually see that the F atom plus the H_2 COM kinetic energies account for most of the 351 meV value of our CASSCF energy barrier (which has been adjusted upward by 26 meV thermal energy at 100 K). The H_2 vibrational energy is also larger than the values in Table 3, and the reason is the small increase in the H–H bond distance at the saddle point when compared with the anion and H_2 equilibrium geometries. Finally, we see that there is a substantial increase in the mean H_2 rotational energy. This increase is associated with the bent TS. This means that the H_2 rotational motion is getting more coupled to

Table 4
Asymptotic fragments obtained for the forward and backward propagation in the neutral PES for trajectories starting from the FH_2 TS

Run	Forward	Backward
$T = 100$ K		
1	HF+H	$F+H_2$
2	$F+H_2$	HF+H
3	HF+H	$F+H_2$
4	$F+H_2$	HF+H
5	HF+H	$F+H_2$
6	$F+H_2$	HF+H
7	$F+H_2$	HF+H
8	HF+H	$F+H_2$
9	HF+H	$F+H_2$
10	HF+H	$F+H_2$

Table 5
Asymptotic energies (meV) for the fragments reported in Table 4

Run	$F+H_2$				HF+H			
T = 100 K	KE_{atom}	KE_{COM}	E_{vib}	E_{rot}	KE_{atom}	KE_{COM}	E_{vib}	E_{rot}
1	27.9	264.8	45.2	27.1	290.0	14.5	1667	3.3
2	29.2	277.8	49.0	9.0	269.5	13.5	1691	0.8
3	28.7	272.7	49.7	14.0	292.8	14.6	1666	1.1
4	27.5	261.4	42.8	33.1	293.8	14.7	1660	5.0
5	25.2	239.5	39.3	58.9	411.2	20.6	1520	21.2
6	26.8	254.9	41.9	41.3	322.9	16.1	1625	7.4
7	31.3	297.0	25.3	11.7	323.5	16.2	1633	0.004
8	30.7	291.8	2.8	39.7	316.6	15.8	1604	39.0
9	31.5	299.3	24.8	9.5	324.6	16.2	1633	0.1
10	34.3	325.6	2.6	1.9	311.5	15.6	1635	7.4
Average	29.3	278.5	32.3	24.6	315.6	15.8	1633	8.5
σ[a]	2.5	24.0	16.9	17.4	36.2	1.8	45	11.8

See Table 3 for definitions.
[a] σ, standard deviation.

the reaction coordinate, and the more bent the TS the bigger the coupling. Therefore, for the TS geometry reported by Stark and Werner [18] (which is probably very close to the true TS) we would expect a highly non-thermal H_2 rotational energy.

The results from Table 5 for the HF + H fragments are strikingly different. First we note that the HF vibrational energy accounts for most of the $\sim$ 1930 meV of exothermicity calculated at our CASSCF level. This is a result of the very stretched HF bond at the TS (we obtain an HF equilibrium bond length of $\sim$ 0.997 Å to be compared with the value of $\sim$ 1.438 Å at the TS). Therefore the HF molecules will be highly excited. The rest of the exothermicity goes basically to the HF COM and H atom translational kinetic energies. The requirement that the total linear momentum is zero now gives $KE_H = 20KE_{COM}$, which agrees very well with the results in Table 5. We see that the light H atom now acquires most of the kinetic energy. Our result for the HF rotational energy has a very large standard deviation, but we can see that the bent TS has less of an effect for the HF rotational energy. This is probably related to the fact that the F atom is much heavier than the H atom, and most of the energy goes into the motion of the dissociated H atom.

In summary, the data in Table 5 demonstrates that the most effective coordinate into which energy should be put to achieve reaction is the H_2 COM translation. Examination of Table 3 reveals that none of the trajectories at 100 K have the necessary H_2 COM translational kinetic energy in order for the reaction to occur. This is yet another reason that the anion-originated trajectories did not produce HF. In order to achieve this analogous situation in $(FH_2)^-$, one would need to excite the (F^-)–H_2 stretching mode.

4. Discussion

As can be seen from Table 2, all the 100 K simulations that started from the anion geometry after the photodetachment had as asymptotic fragments the F atom and H_2 molecule. As discussed in Section 2, this is a consequence of the large F–H bond distance in the anion equilibrium geometry. Every time the anion is excited to the neutral PES, it lands in the reactants valley. As the temperature is much smaller than the reaction barrier it cannot cross classically to the products valley, and the outcome of the simulation is always the $F + H_2$ fragments. For the higher temperature simulations, we see that the system can

now cross to the products side and we obtain FH + H as a possible outcome, even though not all trajectories are reactive, as discussed in the previous section. The results starting from the TS geometry are completely different. All the trajectories propagated forward in time give as final fragments F + H_2 or FH + H, and when they are propagated backwards they give the corresponding other fragments, i.e. FH + H or F + H_2. This is the expected behavior for a true TS. Therefore the conclusion that we reach from our simulation is that the electron photodetachment experiment is not probing the TS region well. Now, the question is how well this conclusion reflects reality.

As discussed in Section 2 the calculation of the FH_2 PES is very difficult. An accurate, quantitative description of the PES requires a much higher level of approximation for the wavefunction than is used in our work. This is also true for the anion PES. For example, the very large F–H bond length in the anion is probably an artifact of our calculation. CCSD(T) theory [29] predicts a much shorter bond, and while it is hard to compare this single reference correlation approach to CASSCF, it is likely that our bond is too long. Based on this fact one would tend to say that the conclusion above regarding whether $(FH_2)^-$ resembles the TS is a pure artifact of our approximations. A closer look, however, indicates that the situation is not so bad. Let us first look at the vibrational frequencies for the anion normal modes. The frequencies calculated by Nichols et al. [29] at the CASSCF level are reported in Table 6. As can be seen there is a very soft $H_2\cdots F^-$ stretching mode, a more stiff bending mode, and the very stiff H–H vibrational mode. Therefore it is easier to stretch/compress the F–H bond than to bend the

Table 6
Vibrational frequencies at the equilibrium geometry for the $(FH_2)^-$ anion calculated by Nichols et al. [29] at the CASSCF level

$H_2\cdots F^-$ stretch	HH stretch	Bending motion
292	4143	773

All values are in cm^{-1}.

Table 7
Energy changes on the anion PES when distorting from the anion equilibrium geometry to the FH_2 TS geometry

	$\Delta V_{F\text{-}H}$	$\Delta V_{H\text{-}H}$	$\Delta V_{\theta_{F\text{-}H\text{-}H}}$
This work	87	14	2
Using Refs. [18,29]	7	0.09	230

All energies are in meV.

F–H–H bond. Now let's look at some numbers. If we use Nichols et al. [29] work as the best values for the anion geometry, and Stark and Werner's [18] structure as the best geometry for the neutral TS, we see that to go from the anion equilibrium geometry (which is linear), to the neutral TS geometry the F–H–H angle has to bend by $\sim 60°$, the F–H bond has to change from 1.690 to 1.541 Å (a compression of 0.149 Å) and the H–H bond distance basically does not change (a small change of 0.002 Å). In our calculation the F–H–H angle has to change only by $\sim 6°$, the F–H bond has to change by 0.559 Å, and the H–H bond changes by 0.03 Å. Some simple estimates [32] give the formulas:

$$V_{F\text{-}H} = 0.29(\Delta R_{F\text{-}H})^2$$

$$V_{H\text{-}H} = 15.9(\Delta R_{H\text{-}H})^2$$

$$V_{\theta_{F\text{-}H\text{-}H}} = 0.21(\Delta\theta_{F\text{-}H\text{-}H}). \quad (2)$$

where $V_{F\text{-}H}$, $V_{H\text{-}H}$, and $V_{\theta_{F\text{-}H\text{-}H}}$ are the harmonic potentials for the F–H stretching, H–H stretching, and F–H–H bending, respectively. The constants are obtained from the calculated frequencies by Nichols et al. (see Table 6) and simple considerations about the effective masses for each mode [32]. $\Delta R_{F\text{-}H}$, $\Delta R_{H\text{-}H}$, and $\Delta\theta_{F\text{-}H\text{-}H}$ are the changes away from equilibrium for the F–H bond, H–H bond, and F–H–H angle, respectively. The constants were calculated in eV $Å^{-2}$ or eV rad^{-2}. Therefore, if the displacements are given in Å or radians, the energies are in eV.

If we now use the above formulas together with the required changes in geometries to get from the anion equilibrium configuration to the neutral TS, we obtain the results shown in Table 7. As can be seen, in our calculations the most costly change is to compress the F–H bond, as discussed above. It

takes a temperature of approximately 1000 K for the F–H bond to get close to the neutral TS in our level of approximation. This agrees qualitatively with the higher temperature simulations that give as outcome the FH + H fragments. Therefore it seems that the higher temperature has the effect of allowing the anion to probe its own PES more effectively to jump closer to the neutral TS configuration instead of providing enough kinetic energy to climb over the neutral surface barrier once on the neutral PES. Now, for the more accurate numbers of Nichols et al. [29] and Stark and Werner [18] we conclude that the most costly change is the bending of the F–H–H angle (it would require a temperature of ~ 2600 K for the anion to bend by $\sim 60°$). Therefore we could conclude that for the real system, even if the anion F–H bond length is not very different from the neutral TS value, *the fact that the anion is linear positions it mostly in the reactants valley and away from the neutral TS.* However, one needs to be more careful. If we examine Stark and Werner's PES for the neutral molecule around the barrier region, for the case where they obtain a bent TS (Fig. 7 in Ref. [18]), we can see that along the linear molecule cut (i.e. F–H–H angle always equal to 180°) the F–H bond in the anion equilibrium geometry is only ~ 0.1 Å away from the products side (it would have to compress from ~ 1.7 to ~ 1.6 Å). According to Eq. (2) this would require an energy of only $\sim$ 3 meV or a temperature of ~ 30–40 K. This is within the range of temperatures used by the experimentalists in their photodetachment experiments. This would mean that it is possible for the anion to be excited into the products valley without bending the F–H–H angle and without ever traversing the actual saddle point! The neutral molecule generated by the photodetachment would still be relatively far from the true TS, but FH + H fragments would still be observed.

There is one last caveat. If the anion FH stretching potential is very anisotropic (which probably is the case), the average F–H bond in the anion will be larger than the calculated equilibrium value (which corresponds to the bottom of the well). This would imply that the anion geometry would have a larger F–H bond on average, which would be closer to our results, and would imply that the FH + H fragments might not be observed even traversing the linear cut on the PES. As a final point, we should stress that tunneling would also contribute to the formation of the FH + H species. If a detailed analysis of the anion PES shows a large anharmonicity and a small probability of forming FH + H, and experimentally it is found that FH + H is easy to form, we must then conclude that tunneling is playing a major role in the process. Evidence that the anharmonicity might be playing an important role is the fact that when anharmonicity is included explicitly by Manolopoulos in his simulations, via a $(FH_2)^-$ ab initio PES calculated by Werner and coworkers (unpublished results), evidence for HF formation via tunneling disappears (D.E. Manolopoulos, private communication).

The experiments in Neumark's group did not record the asymptotic fragments, therefore we cannot make a direct comparison with experiment. It would be very interesting to have an analysis of the final states to clarify the points discussed above and to compare with our results from Tables 2 and 3. However, analysis of the experimental photoelectron spectrum [9–11,20] shows that it is dominated by a bending progression associated with hindered H_2 rotational motion. This has always been connected to the fact that the neutral TS is bent. However, even though there is a change of ~ 0.15 Å in the F–H bond when going from the anion equilibrium geometry to the neutral TS, and an even greater change as the molecule moves toward the products valley, there is no clear sign in the photoelectron spectrum of peaks associated with the FH vibration. This may still support the notion that most, if not all, of the molecules are being excited in the reactants valley, as discussed above. Only an analysis of the asymptotic fragments could resolve this issue.

5. Conclusions

In summary, we have performed the first ab initio molecular dynamics study of a gas phase reaction with a correlated wavefunction, and in

particular the first ab initio molecular dynamics simulation of an electron detachment experiment. We have modeled the photoexcitation process as a sudden jump from the anion PES to the neutral PES. We have shown that AIMD is a good tool to study this type of process because it does not require the knowledge of the whole PES and gives a very nice picture of the dynamics. It does not directly give the anion spectrum, but it helps to identify into which regions of the neutral PES the anion will be excited to, and it provides an easy way to analyse the asymptotic fragments after the photodetachment. However, one has to be careful in the interpretation of the results. The quality of the results obviously will depend of the level of the ab initio calculation that is being used in the calculation of electronic energies and gradients. If the problem under study is not well described at the chosen level, the results may not reflect the true physics. The present work on the FH_2 system is a very tough case because the PES of FH_2 is very hard to calculate at the ab initio level (due to the tiny reaction barrier). However, even in this case, after careful comparison with experiment and with other ab initio PES calculations, it was shown that our AIMD provides a qualitatively correct description of the photodetachment process. For less problematic systems, AIMD will surely be of great value in providing qualitative, and in some cases even quantitative, understanding. Indeed it may be the only means of carrying out ab initio dynamics, as quantum dynamics studies are limited at present (due to computational limitations) to at most six degrees of freedom [33] and the number of highly accurate ab initio PESs that exist are also extremely limited. The beauty of AIMD is the ability to apply it generally and without the pain of fitting an ab initio PES to a functional form, which itself may impose artificial limitations on the dynamics observed. Of course the expense of AIMD will still limit its impact, because of the inability to gather enough statistics.

In the specific case of the FH_2 system, at our level of approximation, we concluded that the anion favors the reactants channel. The asymptotic fragments after electron detachment will mostly be F and H_2, the main reason being the large F–H bond in the anion. In the real situation, the anion geometry also favors the entrance channel, but the reason is the large F–H–H angle in the neutral TS (although a large anharmonicity in the FH stretching potential may also lead to a large average F–H bond for the anion). This leads to similar qualitative behavior between our simulation and experiments. However, the possibility of reaching the exit channel through the linear molecule cut of the PES and bypassing the TS entirely, as well as tunneling (which is not included in the AIMD method) may give a different picture. Comparison with existing experimental data does not answer these questions unequivocally because the asymptotic fragments were not recorded. However, the fact the anion photoelectron spectrum mainly shows an F/H_2 bending progression is a hint that the anion is always being excited into the reactants valley. We suggest that the experimental analysis of the asymptotic fragments, after the photodetachment has occurred, can provide important clues that will help to answer the above questions.

Acknowledgements

This research was supported by the Office of Naval Research. E.A.C. also acknowledges support from the Alfred P. Sloan and Camille and Henry Dreyfus Foundation via Research Fellow and Teacher–Scholar Awards, respectively. Stimulating discussions with Dr David Manolopoulos, Professor Hans-Joachim Werner, Dr Don Arnold, and Professor Daniel Neumark, are gratefully acknowledged.

References

[1] E. Wurzberg and P.L. Houston, J. Chem. Phys., 72 (1980) 4811.
[2] R.F. Heidner III, J.F. Bott, C.E. Gardner and J.E. Melzer, J. Chem. Phys., 72 (1980) 4815.
[3] R. Atkinson, D.L. Baulch, R.A. Cox, R.F. Hampson Jr., S.A. Ferr and J. Troe, J. Phys. Chem. Ref. Data, 18 (1989) 88.
[4] D.M. Neumark, A.M. Wodtke, G.N. Robinson, C.C. Hayden and Y.T. Lee, J. Chem. Phys., 82 (1985) 3045.

[5] D.M. Neumark, A.M. Wodtke, G.N. Robinson, C.C. Hayden, K. Shobatake, R.K. Sparks, T.P. Schafer and Y.T. Lee, J. Chem. Phys., 82 (1985) 3067.
[6] M. Faubel, B. Martínez-Haya, L.Y. Rusin, U. Tappe, J.P. Toennies, F.J. Aoiz and L. Bañares, Chem. Phys., 207 (1996) 245.
[7] F.J. Aoiz, L. Bañares, M. Faubel, B. Martínez-Haya, L.Y. Rusin, U. Tappe and J.P. Toennies, Chem. Phys., 207 (1996) 227.
[8] M. Faubel, L.Y. Rusin, S. Schlemmer, F. Sondermann, U. Tappe and J.P. Toennies, J. Chem. Phys., 101 (1994) 2106.
[9] A. Weaver, R.B. Metz, S.E. Bradforth and D.M. Neumark, J. Chem. Phys., 93 (1990) 5352.
[10] S.E. Bradforth, D.W. Arnold, D.M. Neumark and D.E. Manolopoulos, J. Chem. Phys., 99 (1993) 6345.
[11] D.E. Manolopoulos, K. Stark, H.-J. Werner, D.W. Arnold, S.E. Bradforth and D.M. Neumark, Science, 262 (1993) 1852.
[12] H.F. Schaefer III, J. Phys. Chem., 89 (1985) 5336, and references therein.
[13] C.W. Baushlicher, Jr., S.P. Walch, S.R. Langhoff, P.R. Taylor and R.L. Jaffe, J. Chem. Phys., 88 (1988) 1743.
[14] P.J. Knowles, K. Stark and H.-J. Werner, Chem. Phys. Lett., 185 (1991) 555.
[15] F.J. Aoiz, L. Bañares, V.J. Herrero, V.S. Rábanos, K. Stark and H.-J. Werner, J. Phys. Chem., 98 (1994) 10665; Chem. Phys. Lett., 223 (1994) 215.
[16] E. Rosenman, S. Hochman-Kowal, A. Persky and M. Baer, J. Phys. Chem., 99 (1995) 16523; Chem. Phys. Lett., 239 (1995) 141.
[17] M. Baer, M. Faubel, B. Martinez-Haya, L.Y. Rusin, U. Tappe, J.P. Toennies, K. Stark and H.J. Werner, J. Chem. Phys., 104 (1996) 2743.
[18] K. Stark and H.-J. Werner, J. Chem. Phys., 104 (1996) 6515, and references therein.
[19] J.F. Castillo, D.E. Manolopoulos, K. Stark and H.J. Werner, J. Chem. Phys., 104 (1996) 6531.
[20] C.L. Russel and D.E. Manolopoulos, Chem. Phys. Lett., 256 (1996) 465.
[21] D.M. Neumark, Acc. Chem. Res., 26 (1993) 33.
[22] R.B. Metz, S.E. Bradforth and D.M. Neumark, Adv. Chem. Phys., 81 (1992) 1.
[23] M.P. Allen and D.J. Tildesley, Computer Simulation of Liquids, Clarendon Press, Oxford, 1987.
[24] T.J. Martinez and R.D. Levine, Chem. Phys. Lett., 259 (1996) 252.
[25] R. Car and M. Parrinello, Phys. Rev. Lett., 55 (1985) 2471.
[26] B. Hartke and E.A. Carter, Chem. Phys. Lett., 189 (1992) 358; B. Hartke and E.A. Carter, J. Chem. Phys., 97 (1992) 6569; B. Hartke and E.A. Carter, Chem. Phys. Lett., 216 (1993) 324; B. Hartke, D.A. Gibson and E.A. Carter, Int. J. Quantum Chem., 45 (1993) 59; D.A. Gibson and E.A. Carter, J. Phys. Chem., 97 (1993) 13429; Z. Liu, L.E. Carter and E.A. Carter, J. Phys. Chem., 99 (1995) 4355; D.A. Gibson, I.V. Ionova and E.A. Carter, Chem. Phys. Lett., 240 (1995) 261; D.A. Gibson and E.A. Carter, Mol. Phys., 89 (1996) 1265.
[27] T.H. Dunning, Jr., J. Chem. Phys., 90 (1989) 1007; R.A. Kendall, T.H. Dunning, Jr. and R.J. Harrison, J. Chem. Phys., 96 (1992) 6796.
[28] M. Dupuis, A. Marquez and E.R. Davidson, HONDO 95.3 from CHEM-Station, 1995, IBM Corporation, Neighborhood Road, Kingston, NY 12401.
[29] J.A. Nichols, R.A. Kendall, S.J. Cole and J. Simons, J. Phys. Chem., 95 (1991) 1074.
[30] I.V. Ionova and E.A. Carter, J. Chem. Phys., 98 (1993) 6377.
[31] W.C. Swope, H.C. Andersen, P.H. Berens and K.R. Wilson, J. Chem. Phys., 76 (1982) 637.
[32] G. Herzberg, Molecular Spectra and Molecular Structure II. Infrared and Raman Spectra of Polyatomic Molecules, Van Nostrand, New York, 1945, p. 173.
[33] A. Gross, S. Wilke and M. Scheffler, Phys. Rev. Lett., 75 (1995) 2718; R. Kosloff, in R.E. Wyatt and J.Z. Zhang (Eds.), Dynamics of Molecules and Chemical Reactions, Marcel Dekker, NY, 1996, pp. 185–230.